An Engineered Membrane to Measure Electroporation: Effect of Tethers and Bioelectronic Interface

William Hoiles,[1] Vikram Krishnamurthy,[1,*] Charles G. Cranfield,[2,3] and Bruce Cornell[4]

[1]Department of Electrical and Computer Engineering, University of British Columbia, Vancouver, British Columbia, Canada; [2]School of Medical and Molecular Biosciences, University of Technology Sydney, Broadway, New South Wales, Australia; [3]Victor Chang Cardiac Research Institute, Darlinghurst, New South Wales, Australia; and [4]Surgical Diagnostics, Roseville, New South Wales, Australia

TABLE S1: Parameter Values for $\mathbf{G_p}$ and $\mathbf{W_{es}}$ Numerical Predictions

Symbol	Definition	Value
$c^{\mathrm{Na}}\|_{t=0}$	Initial Na+ concentration	321.45 mol/m^3
$c^{\mathrm{K}}\|_{t=0}$	Initial K+ concentration	13.39 mol/m^3
$c^{\mathrm{Cl}}\|_{t=0}$	Initial Cl− concentration	334.84 mol/m^3
a_{Na}	Na+ effective ion size	4 Å
a_{K}	K+ effective ion size	5 Å
a_{Cl}	Cl− effective ion size	4 Å
D_w^{Na}	Na+ electrolyte diffusion coefficient in Ω_w	1.33×10^{-9} m^2/s
D_w^{K}	K+ electrolyte diffusion coefficient in Ω_w	1.96×10^{-9} m^2/s
D_w^{Cl}	Cl− electrolyte diffusion coefficient in Ω_w	2.07×10^{-9} m^2/s
ε_w	Electrolyte electrical permittivity	7.083×10^{-10} F/m
ε_m	Membrane electrical permittivity	1.771×10^{-11} F/m
F	Faraday constant	9.6485×10^4 C/mol
C_s	Stern layer capacitance	1 pF
k_B	Boltzmann constant	$1.3806488 \times 10^{-23}$ J/K
T	Temperature	300 K
ϕ_e	Electrode potential	100-500 mV
ϕ_{ec}	Counter electrode potential	0 mV
l_r	Tether reservoir length	400 nm
h_r	Tether reservoir height	4 nm
h_m	Membrane thickness	4 nm
h_e	Electrolyte height	60 nm

In Table S1, the concentrations match those used in the electrolyte solution of the engineered tethered membrane. The choice of effective ion size (i.e. solvated ionic radius) is based on the mobility measurements reported in (7, 8). The diffusion coefficients of the ions and electrical permittivities of water and biological membrane are provided in (6). The geometric parameters h_r and h_m are selected to match the experimentally measured results obtained from neutron-reflectometry measurements of similar engineered tethered membranes reported in (1).

TABLE S2: Parameter Values for Current Predictions

Symbol	Definition		Value		
γ	Edge energy		1.8×10^{-11} J/m		
σ	Surface tension		1×10^{-3} J/m^2		
C	Steric repulsion constant		9.67×10^{-15} J$^{1/4}$ m		
D	Radial diffusion coefficient		1×10^{-14} m^2/s		
α	Creation rate coefficient		1 Gs^{-1} $\left[10\ \text{Ms}^{-1} - 0.1\ \text{Ts}^{-1}\right]$		
q	$q = (r_m/r_*)^2$ with the symbols defined below Eq. 17		2.46±0.07		
DphPC Membrane		**Tether Density:**	**1%**	**10%**	**100%**
G_0	Initial membrane conductance		1.67±0.3 μS	0.91±0.04 μS	0.43±0.03 μS
C_m	Membrane capacitance		10.5±0.8 nF	10.5±0.7 nF	11.0±0.2 nF
R_e	Electrolyte resistance		3.5±2 kΩ	3.5±2 kΩ	5.0±3.0 kΩ
C_{dl}	Total electrode double-layer capacitance		136.3±6 nF	136.3±8 nF	118.2±8 nF
V_{ep}	Characteristic voltage of electroporation		430±5 mV	430±5 mV	580±10 mV
N_o	Equilibrium pore density $G_0/G_p(r_m)$		1068 [120-15k]	582 [90-10k]	275 [42-43k]
K_t	Spring constant		0 N/m	2±1.5 mN/m	20±15 mN/m
DphPC Membrane (Reservoir Double-Layer Effect)		**Tether Density:**	**1%**	**10%**	
G_0	Initial membrane conductance		1.00±0.1 μS	1.00±0.1 μS	
C_m	Membrane capacitance		14.6±0.1 nF	16.0±0.4 nF	
R_e	Electrolyte resistance		1.0±0.5 kΩ	1.0±0.5 kΩ	
C_{dl}	Total electrode double-layer capacitance		65±3 nF	39±2 nF	
V_{ep}	Characteristic voltage of electroporation		366±6 mV	400±5 mV	
N_o	Equilibrium pore density $G_0/G_p(r_m)$		641 [100-2k]	641 [100-50k]	
K_t	Spring constant		0 N/m	2±1.5 mN/m	

S1 Impedance Measurement of Tethered Membrane

For a low voltage (i.e. below 50 mV) sinusoidal potential defined by $V_s(t) = V_o \sin(2\pi f)$, where f is the frequency of excitation and V_o is the magnitude of excitation, the impedance of the engineered tethered membrane is given by:

$$Z(f) = R_e + \frac{1}{G_o + j2\pi f C_m} + \frac{1}{j2\pi f C_{dl}} \tag{S1}$$

with the parameters R_e, G_o, C_m, C_{dl} defined in Eq. 1. In Eq. S1, j denotes the complex number $\sqrt{-1}$. To test the quality of the formed membrane we utilize impedance measurements of the membrane and estimate the parameters in Eq. S1. The numerically predicted and measured impedance values are provided in Fig.S1 and Fig.S2. As seen, the predicted impedance is in excellent agreement with the experimental measured impedance and is consistent with a membrane containing negligible defects as discussed in the paper.

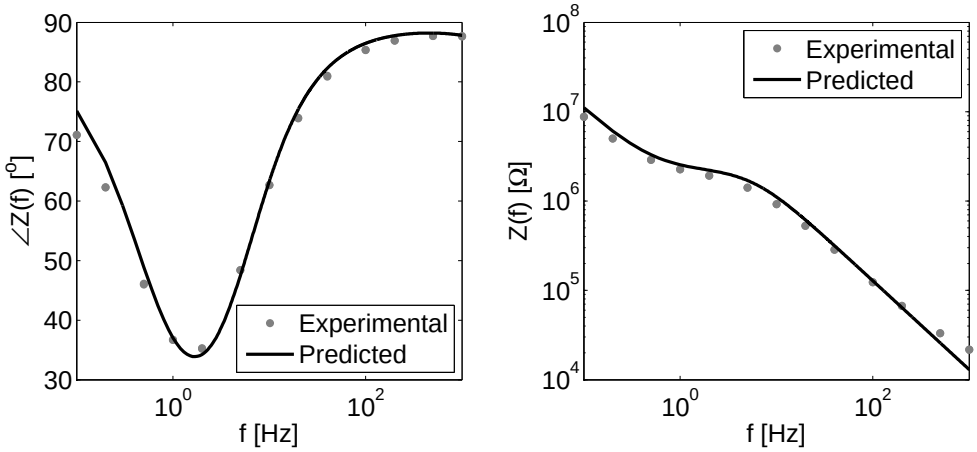

Figure S1: The measured and predicted impedance of the 10% tether density DphPC bilayer membrane. All predictions are computed using Eq. S1 with the parameters defined in Table S2 of the Supporting Material.

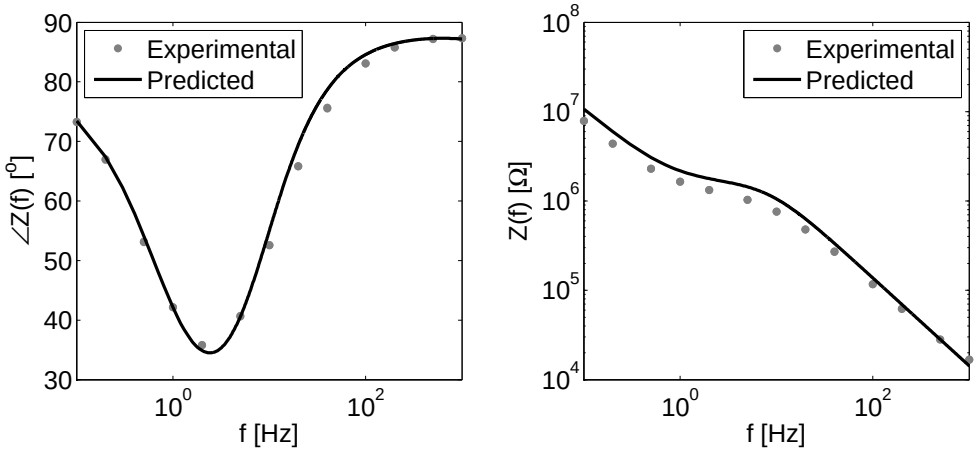

Figure S2: The measured and predicted impedance of the 1% tether density DphPC bilayer membrane. All predictions are computed using Eq. S1 with the parameters defined in Table S2.

S2 Numerical Methods

The numerical estimate of $I(t)$ is computed using Eq. 1 and 2 assuming there are a finite number of possible pore radii using the algorithm presented in (2, 3). The governing equations Eq. 5 with boundary conditions Eq. 8-11, are solved numerically with the com-

mercially available finite element solver COMSOL 4.3a (Comsol Multiphysics, Burlington, MA). To solve the GPNP and PNP models the COMSOL modules *Transport of Diluted Species* and *Electrostatics* are utilized; and to solve the EM model the modules *Nernst-Planck* and *Electrostatics* are utilized. The simulation domain is meshed with approximately 270,000 triangular elements constructed using an advancing front meshing algorithm. The GPNP and PNP are numerically solved using the *multifrontal massively parallel sparse direct solver* (4) with a variable-order variable-step-size backward differential formula (5). Eq. 12 is used to compute the pore conductance with the integration done in the region defined in Fig. 3. The conductance is computed for a finite number of equally spaced radii between 0.5-10 nm with a step-size of 0.25 nm. The steady-state conductance G_p, Eq. 12, is estimated when the percentage change in conductance between successive steps (i.e. $|(G_p(t_{i+1}) - G_p(t_i))/G_p(t_i)|$) is less then 1%. The total force acting on the toroidal pore $F(r)$, Eq. 16, is computed using the results from the conductance computation. Substituting $F(r)$ into Eq. 13, the total electrical energy required to form the pore W_{es} is computed.

Supporting References

[1] Heinrich, F., T. Ng, D. Vanderah, P. Shekhar, M. Mihailescu, H. Nanda, and M. Losche, 2009. A new lipid anchor for sparsely tethered bilayer lipid membranes. *Langmuir* 25:4219–4229.

[2] Smith, K., J. Neu, and W. Krassowska, 2004. Model of creation and evolution of stable electropores for DNA delivery. *Biophysical Journal* 86:2813 – 2826.

[3] Krassowska, W., and P. Filev, 2007. Modeling electroporation in a single cell. *Biophysical Journal* 92:404 – 417.

[4] Amestoy, P., I. Duff, J. L'Excellent, and J. Koster, 2001. A fully asynchronous multifrontal solver using distributed dynamic scheduling. *SIAM Journal on Matrix Analysis and Applications* 23:15–41.

[5] Brown, P., A. Hindmarsh, and L. Petzold, 1994. Using Krylov methods in the solution of large-scale differential-algebraic systems. *SIAM Journal on Scientific Computing* 15:1467–1488.

[6] Hobbie, R., and B. Roth, 2007. Intermediate physics for medicine and biology. Springer.

[7] Nightingale, E., 1959. Phenomenological theory of ion solvation. Effective radii of hydrated ions. *The Journal of Physical Chemistry* 63:1381–1387.

[8] Israelachvili, J., 2011. Intermolecular and surface forces: revised third edition. Academic press.